

# A model of glueballs

Roman V. Buniy and Thomas W. Kephart  
*Department of Physics and Astronomy*  
*Vanderbilt University, Nashville, TN 37235*

## Abstract

We model the observed glueball mass spectrum in terms of energies for tightly knotted and linked QCD flux tubes. The data is fit well with one parameter. We predict additional glueball masses.

*Introduction.*— The interpretation of non- $q\bar{q}$  states is a puzzle with a long and controversial history [1]. Many experiments [2] report states that do not fit neatly into the quark model. These states can be broadly classified as: (1) hybrids, which are bound states of quarks and gluons like  $q\bar{q}G$  with quantum numbers  $J^{PC} = 0^{-+}, 1^{-+}, 1^{--}, 2^{-+}, \dots$ ; (2) exotics, for example, four and six quark states such as  $qq\bar{q}\bar{q}$  and  $qqq\bar{q}\bar{q}\bar{q}$  with quantum numbers  $J^{PC} = 0^{--}, 0^{+-}, 1^{-+}, 2^{+-}, \dots$ ; (3) glueballs with pointlike or collective (e.g., strings à la Nielsen–Olesen [3], or flux tubes) glue. Glueballs do not contain valence quarks, but there could be sea/virtual quarks within the glueball or in the currents that support the flux tubes. From a bag model perspective one is led to suppose that the lightest non- $q\bar{q}$  states are those with no constituent quarks, i.e., the glueballs. Lattice calculations, QCD sum rules, electric flux tube models, and constituent glue models leads to a consensus that the lightest non- $q\bar{q}$  states are glueballs with quantum numbers  $J^{++} = 0^{++}$  and  $2^{++}$  [4]. We will model all  $J^{++}$  states (i.e., all  $f_J$  and  $f'_J$  states listed by the Particle Data Group (PDG) [2]), some of which will be identified with rotational excitations, as knotted/linked chromoelectric QCD flux tubes [5].

Besides the fact they do not fit in the quark model [6], glueballs have some other characteristic signatures, including: enhanced central production in gluon rich channels, branching fractions incompatible with  $q\bar{q}$  decay, reduced  $\gamma\gamma$  coupling, and OZI suppression. All the  $J^{++}$  states we consider have some or all of these properties. For instance, none have substantial branching fractions to  $\gamma\gamma$ . However, mixing with  $q\bar{q}$  isoscalar states can obscure some of the properties. A number of candidates with masses below  $2.5\text{ GeV}$  have been identified. Beyond their masses and widths, and some of their branching ratios [2], much remains to be learned about these states.

Knotted magnetic fields (which we will treat as solitons) have been suggested as candidates for a number of plasma phenomena in systems ranging from astrophysical, to atmospheric [7], to Bose-Einstein condensates [8]. The energies of these solitons are sometimes difficult to quantify since they depend on parameters of the plasma, including temperature, pressure, density, ionic content, etc.; however, we will argue that in QCD a well defined soliton energy can be identified.

As has been shown in plasma physics, tight knots and links (defined below) correspond to metastable minimum energy configurations. We will argue by analogy that quantized tightly knotted and linked QCD flux tubes are glueballs. (In what follows, we often use the term “knots” to mean knots and/or links.)

Movement of fluids often exhibits topological properties (for a mathematical review see e.g. [9]). For conductive fluids, interrelation between fluid motion and magnetic fields via magnetohydrodynamics may cause magnetic fields, in their turn, to exhibit topological properties. For example, for a

perfectly conducting fluid, the (Abelian) magnetic helicity  $L_H = \int d^3x \epsilon_{ijk} A_i \partial_j A_k$  is an invariant of motion [10], and this quantity can be interpreted in terms of knottedness of magnetic flux lines [11].

The dynamics of the magnetic fields follows the dynamics of the liquid (magnetic flux lines are “frozen” into the fluid), and one finds that a perfectly conducting, viscous and incompressible fluid relaxes to a state of magnetic equilibrium without a change in topology [12]. As a result, for topologically non-trivial plasma flows (with knotted streamlines), the “freezing” condition forces topological restrictions on possible changes in field configurations. For linked non-intersecting loops  $C_a$  with magnetic fluxes  $\Phi_a$ , the helicity becomes [11]  $L_H = \frac{k}{8\pi} \sum_{a \neq b} L(C_a, C_b) \Phi_a \Phi_b$ . Here  $L(C_a, C_b)$  is the Gauss linking number [13]. By its topological nature, helicity in the QCD flux can be one of the quantum numbers characterizing glueballs. However, there is another invariant called the knot energy that is less obvious but as important in the classification of solitonic knots.

*Knot energies.* — Consider a hadronic collision that produces some number of baryons and mesons plus a gluonic state in the form of a closed QCD flux tube (or a set of tubes). From an initial state, the fields in the flux tubes quickly relax to an equilibrium configuration, which is topologically equivalent to the initial state. (We assume topological quantum numbers are conserved during this rapid process.) The relaxation proceeds through minimization of the field energy. Flux conservation and energy minimization force the fields to be homogeneous across the tube cross sections. This process occurs via shrinking the tube length, and halts to form a “tight” knot or link. The radial scale will be set by  $\Lambda_{\text{QCD}}^{-1}$ . The energy of the final state depends only on the topology of the initial state and can be estimated as follows. An arbitrarily knotted tube of radius  $a$  and length  $l$  has the volume  $\pi a^2 l$ . Using conservation of flux  $\Phi_E$ , the energy becomes  $\propto l(\text{tr} \Phi_E^2)/(\pi a^2)$ . Fixing the radius of the tube (to be proportional to  $\Lambda_{\text{QCD}}^{-1}$ ), we find that the energy is proportional to the length  $l$ . The dimensionless ratio  $\varepsilon(K) = l/(2a)$  is a topological invariant and the simplest definition of the “knot energy” [14].

Many knot energies have been calculated by Monte Carlo methods [15] and certain types can be calculated exactly (see below), while for other cases simple estimates can be made (see Table 1). For example, the knot energy of the connected product of two knots  $K_1$  and  $K_2$  satisfies

$$\varepsilon(K_1 \# K_2) < \varepsilon(K_1) + \varepsilon(K_2) \quad (1)$$

A rule of thumb is

$$\varepsilon(K_1 \# K_2) \approx \varepsilon(K_1) + \varepsilon(K_2) - (2\pi - 4), \quad (2)$$

which results from removing two half tori, one from each knot, and replacing these with two connecting cylinders of lengths  $a$ . This, for example, agrees with the Monte Carlo values for  $\varepsilon(3_1 \# 3_1)$  and  $\varepsilon(3_1 \# 3_1^*)$  to about 5%.

Most of the knot energies in Table 1 have been taken from [15], but we have independently calculated the energy of  $2_1^2$ ,  $4_1^3$  and  $6_1^4$  exactly and the energy for several other knots and links approximately. We find  $\varepsilon(2_1^2) = 4\pi \approx 12.57$ , to be compared with the Monte Carlo value 12.6. We also find  $\varepsilon(4_1^3) = 6\pi + 2$  and  $\varepsilon(6_1^4) = 8\pi + 3$ , where there are no Monte Carlo comparisons available, or needed.

*Model.* — In our model, the chromoelectric fields [16]  $F_{0i}$  are confined to knotted tubes, each carrying one quantum of conserved flux [17] [18]. We consider a stationary Lagrangian density

$$\mathcal{L} = \frac{1}{2} \text{tr} F_{0i} F^{0i} - V, \quad (3)$$

where, similar to the MIT bag model [19], we included the possibility of a constant energy density  $V$ . To account for conservation of the flux  $\Phi_E$ , we add to (3) the term

$$\text{tr} \lambda \{ \Phi_E / (\pi a^2) - n^i F_{0i} \}, \quad (4)$$

where  $n^i$  is the normal vector to a section of the tube and  $\lambda$  is a Lagrange multiplier. Varying the full Lagrangian with respect to  $A_\mu$ , we find

$$D^0(F_{0i} - \lambda n_i) = 0, \quad D^i(F_{0i} - \lambda n_i) = 0, \quad (5)$$

which has the constant field

$$F_{0i} = (\Phi_E/\pi a^2)n_i \quad (6)$$

as its solution. With this solution, the energy is positive and proportional to  $l$  and thus the minimum of the energy is achieved by shortening  $l$ , i.e. tightening the knot.

We proceed to identify knotted and linked QCD flux tubes with glueballs, where we include all  $f_J$  and  $f'_J$  states. The lightest candidate is the  $f_0(600)$ , which we identify with the shortest knot/link, i.e., the  $2_1^2$  link (see Figure 1); the  $f_0(980)$  is identified with the next shortest knot, the  $3_1$  trefoil knot (see Figure 2), and so forth. All knot and link energies have been calculated for states with energies less than 1680 MeV. Above 1680 MeV the number of knots and links grows rapidly, and few of their energies have been calculated. However, we do find knot energies corresponding to known  $f_J$  and  $f'_J$  states, and so can make preliminary identifications in this region. (We focus on  $f_J$  and  $f'_J$  states from the PDG summary tables. The experimental errors are also quoted from the PDG. There are a number of additional states reported in the extended tables, but some of this data is either conflicting or inconclusive.)

Our detailed results are collected in Table 1, where we list  $f_J$  and  $f'_J$  masses, widths, and our identifications of these states with knots, together with the corresponding knot energies.

In Figure 3 we compare the mass spectrum of  $f$  states with the identified knot and link energies. Since errors for the knot energies in [15] were not reported, we conservatively assumed the error to be 1%. A least squares fit to the most reliable data (below 1680 MeV) gives

$$E(G) = (23.4 \pm 46.1) + (59.1 \pm 2.1)\varepsilon(K) \quad [\text{MeV}], \quad (7)$$

with  $\chi^2 = 9.1$ . The data used in this fit is the first seven  $f_J$  states (filled circles in Figure 3) in the PDG summary tables. Inclusion of the remaining seven (non-excitation) states (unfilled circles in Figure 3) in Table 1, where either the glueball or knot energies are less reliable, does not significantly alter the fit and leads to

$$E(G) = (26.9 \pm 24.9) + (58.9 \pm 1.0)\varepsilon(K) \quad [\text{MeV}], \quad (8)$$

with  $\chi^2 = 10.1$ . The fit (7) is in good agreement [20] with our model, where  $E(G)$  is proportional to  $\varepsilon(K)$ . Better HEP data and the calculation of more knot energies will provide further tests of the model and improve the high mass identification.

In terms of the bag model [19], the interior of tight knots correspond to the interior of the bag. The flux through the knot is supported by current sheets on the bag boundary (surface of the tube). Knot complexity can be reduced (or increased) by unknotting (knotting) operations [21, 22]. In terms of flux tubes, these moves are equivalent to reconnection events [23]. Hence, a metastable glueball may decay via reconnection. Once all topological charge is lost, metastability is lost, and the decay proceeds to completion. Two other glueball decay processes are: flux tube (string) breaking; this favors large decay widths for configurations with long flux tube components; and quantum fluctuations that unlink flux tubes; this would tend to broaden states with short flux tube components. As yet we are not able to go beyond these qualitative observations, but hope to be able to do so in the future.

We have assumed one fluxoid per tube. There may be states with more than one fluxoid, but these would presumably have somewhat fatter flux tubes with higher flux densities and higher energies.

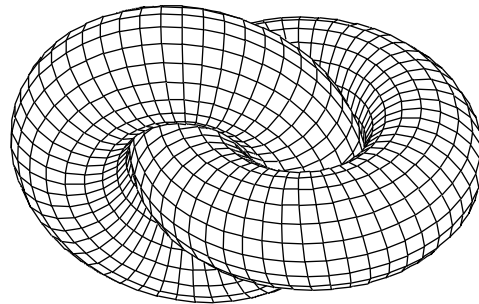


Figure 1: The shortest knot/link solitonic flux configuration has the topology of two linked tori, which in knot theory notation is  $2_1^2$ . This corresponds to the lightest glueball candidate  $f_0(600)$ .

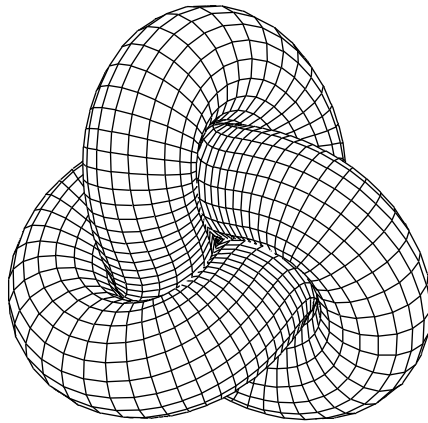


Figure 2: The second shortest solitonic flux configuration is the trefoil knot  $3_1$  corresponding to the second lightest glueball candidate  $f_0(980)$ .

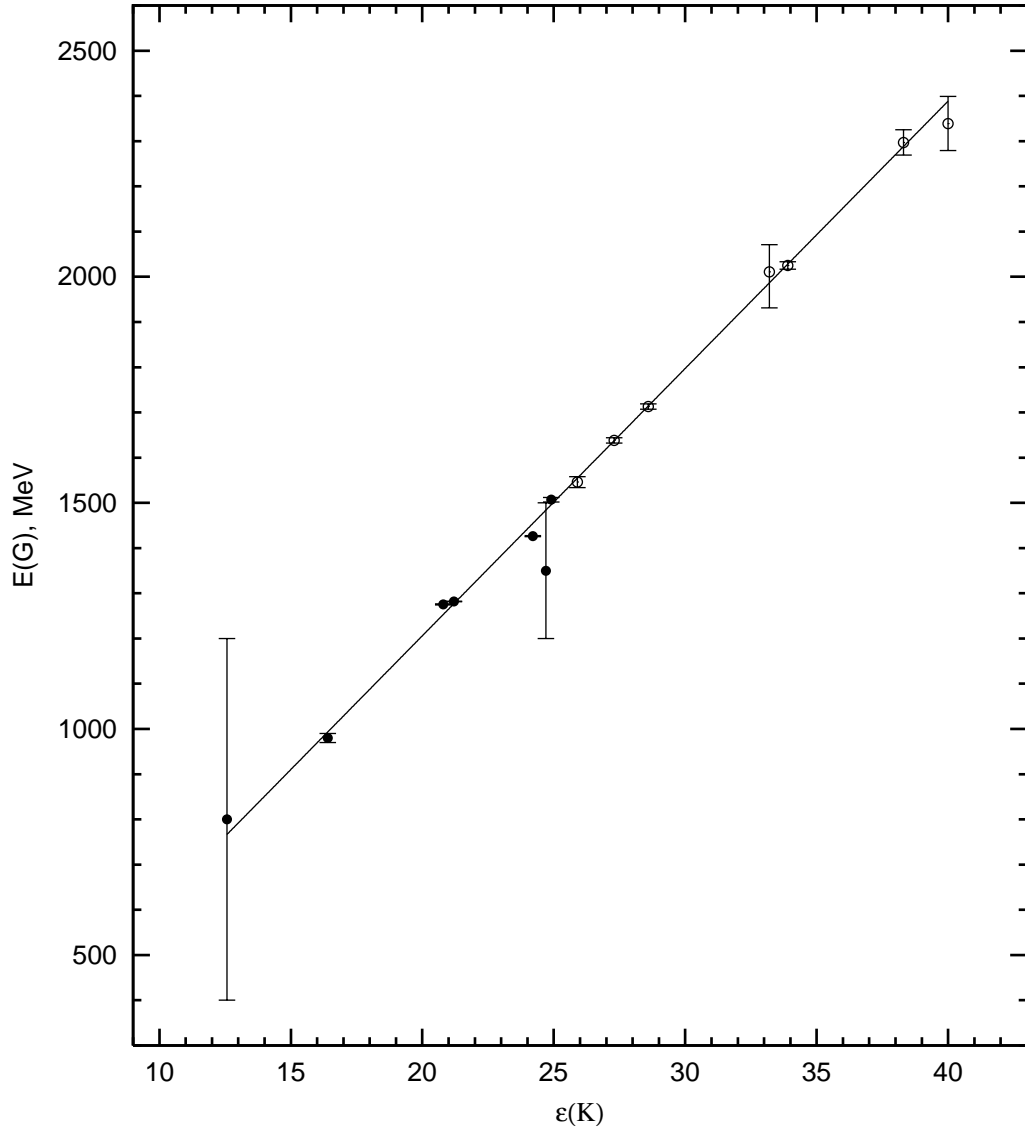


Figure 3: Relationship between the glueball spectrum  $E(G)$  and knot energies  $\epsilon(K)$ . Each point in this figure represents a glueball identified with a knot or link. The straight line is our model and is drawn for the fit (7).

For example, the two fluxoid trefoil knot  $3_1$  would certainly have  $\varepsilon(K) > 2\varepsilon(3_1)$  and a fairly reliable estimate gives  $\varepsilon(K) \approx 2\sqrt{2}\varepsilon(3_1)$ . Hence most multfluxoid states would be above the mass range of known glueballs.

*Discussions and conclusions.*— In principle, lattice calculations can find any tame knot (knot without an infinite number of crossings or other pathology [21]) configuration, since there is always a contour through the lattice that represents the knotted path by some specific Wilson loop. However, since one is constrained by the rigidity of the lattice, energy minimization is difficult and requires a very fine-grained lattice. Thus we expect shape-evolving Monte Carlo techniques [15] to be much more efficient and accurate for this purpose.

Now we must discuss the details of identifications made in Table 1. First, the  $f_2(1270)$  does have a quark model interpretation. Either the glueball state in this range is well mixed with the quark model state and is part of the resonance at 1275 MeV (our interpretation), or the glueball state is yet to be discovered. In either case, more data in this region would be helpful. Next, the four (unconfirmed) glueball states with masses less than 1680 MeV from the extended PDG tables are identified as follows: (1) the  $4_1^2$  link with  $E(G) = 1289$  and the  $4_1$  knot with  $E(G) = 1277$  are nearly degenerate, and the  $f_1(1285)$  could actually be a pair of nearly degenerate states with identical quantum numbers associated with these knots; this is a possible interpretation of the  $f_1(1285)$  mass measurements summarized on page 481 of Ref. [2]; (2) the  $f_2(1430)$  is treated as a rotational excitation of the  $f_1(1420)$  and identified with the  $5_1$  knot; the energy difference between these two states,  $\delta'$ , is a few MeV, but not well determined; this difference is of the order of what one would expect for rotational excitations; [We approximate  $E(f_J) = E(f_0) + \frac{1}{2}J(J+1)\delta$ .] (3) we treat the  $f_1(1510)$  as the first and the  $f_2'(1525)$  could be the second [24] rotational excitation of the  $f_0(1500)$ , which we identify with the  $5_2$  knot; now the energy step size is  $\delta \approx 5\text{MeV}$  which agrees with a simple estimate; (4) we assign the  $f_2(1565)$  and the  $f_2(1640)$  to the  $5_1^2$  and the  $6_3^3$  links respectively.

Further details of knot excitations would be interesting to investigate, as would quantum and curvature corrections. At present we do not have a reliable way to estimate all these effects, nor do we have a good way to calculate glueball decays. However, we do expect high mass glueball production to be suppressed because more complicated non-trivial topological field configurations are statistically disfavored.

Finally, knot solitons may also be able to survive within a quark-gluon plasma (e.g., in the interior of a RHIC event, quark star, or in the early universe). Complications will certainly arise in these cases due to additional parameters describing the media, as with knotted and linked electromagnetic plasma solitons; but if one holds the parameters constant throughout the region of interest in this or any system that supports knot/link solitons, the energy spectrum will be universal up to a scaling.

*Acknowledgments.*— We thank Med Webster, Kevin Stenson, Eric Vaandering, Will Johns, Tom Weiler, and Jack Ng for useful comments and discussions. This work was supported by U.S. DoE grant number DE-FG05-85ER40226.

## References

- [1] E. S. Swanson, *7th International Conference on Hadron Spectroscopy (Hadron 97)*, Upton, NY, AIP Conf. Proc. **432**, 471 (1997).
- [2] K. Hagiwara et al., *Phys. Rev.*, D66, 010001, (2002).
- [3] H. B. Nielsen and P. Olesen, *Nucl. Phys.*, B61, 45 (1973).

- [4] For further discussion of glueballs and their quantum numbers see, for instance G. B. West, *Nucl. Phys. Proc. Suppl.*, 54A, 353 (1997); N. A. Tornqvist, “Summary of Gluonium95 and Hadron95 Conferences,” arXiv:hep-ph/9510256; J. Terning, arXiv:hep-ph/0204012; R. C. Brower, *Int. J. Mod. Phys.*, A16S1C, 1005 (2001); M. Suzuki, *Phys. Rev.*, D65, 097507 (2002); M. Teper, *Nucl. Phys. Proc. Suppl.*, 109, 134 (2002).
- [5] In terms of ’t Hooft’s dual confinement picture, confinement is due to monopole condensation, with flux tubes being chromoelectric. However, since we as yet have no soliton solutions to the full QCD theory, we are not married to any confinement scheme; all we require are tightly knotted/linked flux tubes (chromoelectric, chromomagnetic, or even chromodyonic) of uniform cross section, though we prefer to go with conventional interpretation. One could potentially gain information on confinement from an analysis of glueball decay (see the discussion below). Also, one could potentially model hybrid states or even exotics as knotted/linked color flux tube type bags with valance quarks inside. Although this topic is outside the scope of the current discussion, we hope to address it elsewhere.
- [6] We note that attempts have been made to fit several of the  $f_J^{++}$  states into the quark model.
- [7] A. F. Rañada, M. Soler, and J. L. Trueba, *Phys. Rev.*, E62, 7181 (2000).
- [8] Y. M. Cho, arXiv:cond-mat/0112325.
- [9] V. I. Arnold and B. A. Khesin, *Topological Methods in Hydrodynamics*, Springer, 1998.
- [10] L. Woltier, *Proc. Nat. Acad. Sci.*, 44, 489 (1958).
- [11] H. K. Moffatt, *J. Fluid Mech.*, 159, 117 (1969).
- [12] H. K. Moffatt, *J. Fluid Mech.*, 159, 359 (1985).
- [13] For a conserved non-Abelian helicity [R. Jackiw, V. P. Nair, and So-Young Pi, *Phys. Rev.*, D62, 085018 (2000)], we can identify  $L_H$  with the Chern-Simons Lagrangian [which is also used for knot classification, E. Witten, *Commun. Math. Phys.*, 121, 351 (1989)], and choose the corresponding gauge invariant expression with topological properties,  $L_H = L_{CS} = \text{tr} \int d^3x \epsilon_{ijk} (A_i \partial_j A_k + \frac{2}{3} A_i A_j A_k)$ .
- [14] H. K. Moffatt, *Nature*, 347, 367 (1990); S. G. Whittington, D. W. Sumners, and T. Lodge, editors, *Topology and Geometry in Polymer Science*, Springer, 1998; R. A. Litherland, J. Simon, O. Durumeric, and E. Rawdon, *Topology Appl.*, 91, 233 (1999); G. Buck and J. Simon, *Topology Appl.*, 91, 245 (1999).
- [15] V. Katritch, et al., *Nature*, 384, 142 (1996); V. Katritch, et al., *Nature*, 388, 148 (1997).
- [16] It has been argued that the confinement of color magnetic flux tubes is possible but requires light quarks in the spectrum of the theory [A. S. Goldhaber, Phys. Rept. **315**, 83 (1999)]; hence confinement once again requires the full QCD Lagrangian. To form chromomagnetic flux tubes, we need the analog of Eqs. (3)-(6). The Lagrangian density becomes  $\mathcal{L} = \frac{1}{2} \text{tr} F_{ij} F^{ij} - V$ , to which we add  $\text{tr} \lambda \{ \Phi_B / (\pi a^2) - \frac{1}{2} \epsilon^{ijk} n_i F_{jk} \}$ . Then variation gives  $D^j (F_{ij} - \frac{1}{2} \epsilon_{ijk} n^k \lambda) = 0$  with resulting constant fields  $F_{ij} = (\Phi_B / \pi a^2) \epsilon_{ijk} n^k$ . Again, the energy is positive and proportional to  $l$ .



- [17] In a discussion of flux quantization in non-Abelian gauge theories, it is important to keep the following fact in mind. For a static configuration, and using the temporal gauge, we can avoid the creation of chromomagnetic flux lines inside the flux tubes [3]. The dual argument shows chromoelectric flux creation can be avoided as well.
- [18] For other approaches to solitonic bags see: R. Friedberg and T. D. Lee, *Phys. Rev.*, D18, 2623 (1978); R. Goldflam and L. Wilets, *Phys. Rev.*, D25, 1951 (1982); G. Clement and J. Stern, *Phys. Rev.*, D34, 1581 (1986).
- [19] A. Chodos, R. L. Jaffe, K. Johnson, Charles B. Thorn, and V. F. Weisskopf, *Phys. Rev.*, D9, 3471 (1974); T. DeGrand, R. L. Jaffe, K. Johnson, and J. E. Kiskis, *Phys. Rev.*, D12, 2060 (1975).
- [20] Note that  $\chi^2 = 251$  for a fit where the first glueball is missed out, and  $\chi^2 = 355$  for a fit where the first knot/link is missed out. This is strong evidence that our identification is appropriate.
- [21] D. Rolfsen, *Knots and Links*, Publish or Perish, 1990.
- [22] L. H. Kauffman, *Knots and physics*, World Scientific, 2001.
- [23] E. Priest and T. Forbes, *Magnetic Reconnection: MHD Theory and Applications*, Cambridge, 2000.
- [24] However, there is strong evidence that the  $f'_2(1525)$  fits well into the quark model. If we drop it from our table, the  $\chi^2$  is unaffected since we only fit the ground state knots, not their excitations.

---

<sup>a</sup>Notation  $n_k^l$  means a link of  $l$  components with  $n$  crossings, and occurring in the standard table of links (see e.g. [21]) on the  $k^{\text{th}}$  place.  $K\#K'$  stands for the knot product (connected sum) of knots  $K$  and  $K'$  and  $K * K'$  is the link of the knots  $K$  and  $K'$ .

<sup>b</sup>Values are from [15] except for our exact calculations of  $2_1^2$ ,  $2_1^2 * 0_1$ , and  $(2_1^2 * 0_1) * 0_1$  in square brackets, our analytic estimates given in parentheses, and our rough estimates given in double parentheses.

<sup>c</sup> $E(G)$  is obtained from  $\varepsilon(K)$  using the fit (7).

<sup>d</sup>States in braces are not in the PDG summary tables.

<sup>e</sup>This is the link product that is not  $2_1^2 * 2_1^2$ .

<sup>f</sup>Resonances have been seen in this region, but are unconfirmed [2].

Table 1: Comparison between the glueball mass spectrum and knot energies.

State	Mass	Width	$K$ <sup>a</sup>	$\varepsilon(K)$ <sup>b</sup>	$E(G)$ <sup>c</sup>
$f_0(600)$	400 – 1200	600 – 1000	$2_1^2$	12.6 [4 $\pi$ ]	768 [766]
$f_0(980)$	$980 \pm 10$	40 – 100	$3_1$	16.4	993
$f_2(1270)$	$1275.4 \pm 1.2$	$185.1_{-2.6}^{+3.4}$	$2_1^2 * 0_1$	[6 $\pi$ + 2]	[1256]
$f_1(1285)$	$1281.9 \pm 0.6$	$24.0 \pm 1.2$	$4_1$	21.2	1277
			$4_1^2$	(21.4)	(1289)
$f_1(1420)$	$1426.3 \pm 1.1$	$55.5 \pm 2.9$	$5_1$	24.2	1454
$\{f_2(1430)$	$\approx 1430\}$ <sup>d</sup>		$5_1$	24.2	$1454 + \delta'$
$f_0(1370)$	1200 – 1500	200 – 500	$3_1 * 0_1$	(24.7)	(1484)
$f_0(1500)$	$1507 \pm 5$	$109 \pm 7$	$5_2$	24.9	1496
$\{f_1(1510)$	$1518 \pm 5$	$73 \pm 25\}$	$5_2$	24.9	$1496 + \delta$
$f_2'(1525)$	$1525 \pm 5$	$76 \pm 10$	$5_2$	24.9	$1496 + 3\delta$
$\{f_2(1565)$	$1546 \pm 12$	$126 \pm 12\}$	$5_1^2$	(25.9)	(1555)
$\{f_2(1640)$	$1638 \pm 6$	$99_{-24}^{+28}\}$	$6_3^3$	((27.3))	((1638))
.....					
$f_0(1710)$	$1713 \pm 6$	$125 \pm 10$	$(2_1^2 * 0_1) * 0_1$ <sup>e</sup>	[8 $\pi$ + 3]	[1686] <sup>f</sup>
			$6_2^3$	((28.6))	((1714))
			$3_1 \# 3_1^*$	28.9 (30.5)	1732 (1827)
			$3_1 \# 3_1$	29.1 (30.5)	1744 (1827)
			$2_1^2 * 2_1^2$	[8 $\pi$ + 4]	[1745]
			$6_2$	29.2	1750
			$6_1$	29.3	1756
			$6_3$	30.5	1827
			$7_1$	30.9	1850
			$8_{19}$	31.0	1856
			$8_{20}$	32.7	1957
$f_2(2010)$	$2011_{-80}^{+60}$	$202 \pm 60$	$7_2$	33.2	1986
$f_4(2050)$	$2025 \pm 8$	$194 \pm 13$	$8_{21}$	33.9	2028
			$8_1$	37.0	2211
			$10_{161,162}$	37.6	2247
$f_2(2300)$	$2297 \pm 28$	$149 \pm 40$	$8_{18}, 9_1$	38.3	2288
$f_2(2340)$	$2339 \pm 60$	$319_{-70}^{+80}$	$9_2$	40.0	2389
			$10_1$	44.8	2672
			$11_1$	47.0	2802